

Enhanced Model of Hybrid Controller for Smooth Switching of Energy Sources Used in Electric Vehicle Application

VENKATA KOTESWARA RAO N¹, RAJA SATHISH KUMAR^{2,*},
Y. V. BALARAMA KRISHNA RAO³

¹Department of Electrical and Electronics Engineering,
Stann's college of engineering and technology, Chirala,
Andhra Pradesh- 523187,
INDIA

²Department of Electrical and Electronics Engineering,
Keshav Memorial Institute of Technology,
Hyderabad,
INDIA

³Department of Electrical and Electronics Engineering,
Guru Nanak Institutions Technical Campus, Ibrahimpatnam,
Telangana-501506,
INDIA

Abstract: - The sharing of load current to battery and ultracapacitor (UC) of the multiple energy storage structure (MESS) according to the vehicle dynamics is the main obstacle in the electric vehicles (EVs) application. In this paper, a control strategy technique is projected, to split the current between two sources based on the EVs requirement. A conventional/intelligent controller is used here to produce pulses to the DC-DC converter's corresponding load on the motor. A math condition-based controller (CBC) is designed by considering four individual math functions based on the speed condition of the motor, which is used to produce regulated pulse signals of the switches present in converters. The combination of CBC plus conventional/intelligent controllers makes a new hybrid controller, to achieve the main objective of the proposed work. The performance of the designed control strategy is investigated with four modes based on changed loads. Two different hybrid controllers CBC plus fuzzy logic (FLC) and CBC with proportional integral derivative (PID), and implemented and a comparative analysis was also made based on different time domain specifications by taking the speed curve as a reference.

Key-Words: - Control strategy, electric vehicles, DC-DC converters, Time-domain specifications, condition-based controller (CBC), Proportional integral derivative (PID), Fuzzy logic (FLC) Controller.

Received: August 7, 2023. Revised: February 5, 2024. Accepted: March 1, 2024. Published: April 1, 2024.

1 Introduction

To achieve the proper energy sharing from energy sources of MESS a single variable rate limit function is adopted and based on that function rate limit controller is modeled. With the modeled control mechanism, the life of the key source is improved by transferring the sudden power needed of the load to the auxiliary source. According to the designed controller function, the primary source can serve the load during normal road conditions only which indicates that the secondary source provides support to the primary source, especially during

abnormal load changes and starting of the vehicle, [1], [2].

The optimized fuel economy and driving range are the most effective factor of EVs during the section of the fuel to drive them. Generally, the battery/fuel cell will act as a base source that will not send the mandatory power to the load at all times. Suppose the driving range of the vehicle is improved to 15%, which will affect the cost of the vehicle means the size of the source increases. To overcome that problem, MESS is constructed with UC and battery/fuel cell, [3], [4], [5].

An NMPC (nonlinear model predictive control) is introduced for the MESS to share the energy between the battery and UC in an optimizing way. The intended technique is a real-time controller, which will improve the dynamics of the overall system, [6], [7], [8].

To obtain the optimal current sharing between the battery and UC two different controllers are modeled and implemented in the system. An improved problem is attained from the first controller based on the Karush–Kuhn– Tucker conditions, this will enhance the MESS efficiency by providing the energy to the load depending upon the applied load to the vehicle. And the second controller is formulated based on the neural networks which additionally have an intelligent working future. The state of health (SoH) of the battery has been measured for both the controllers' working times to know the optimal performance of the individual controller. To compare the software-based results, and hardware model has realized. Thereafter a comparative study was done based on Simulink as well as hardware model results for better validation, [9], [10], [11].

A novel MESS is anticipated with two unique character power sources and the energy flow from the sources to load is also controlled with a specific controller. The proposed controller, mainly concentrates on reducing the sudden surge effects on the primary source by diverting to the supporting source. The main converter BDC is used for two ways of current flow with two separate switches for boost and buck operations, [12], [13]. The MESS includes two sources which are battery and UC are connected to the DC bus through converters, to reduce the hardware realization cost. The complete performance of the controller used in this work is examined based on several road conditions. The converters used in this worked effectively for the given power ranges of the load, [14], [15], [16].

Novel MESS is proposed and compared with the existing traditional power storage system. In the selected UC and battery is rated with lower voltages than the bus voltage which reduces the fabrication cost of the overall system. With this arrangement, the normal voltage profile has been developed to the main source battery, by diverting the heavy power development to the UC, [17], [18], [19], [20].

2 Battery-Ultracapacitor Hybrid System Architecture

Figure 1 shows its main concentration on, how to produce the regulated signals to a converter. This includes two converters both are used here to realize the planned control scheme. Of those controllers first, one is the regular one, which is used to generate the switching, signals on the other hand CBC controller, is capable of controlling the pulses made by the conventional controller related to the four math functions ON and OFF states. Here the CBC controller takes input as speed from the electric motor and develops the four math functions as an output related to the speed of the motor.

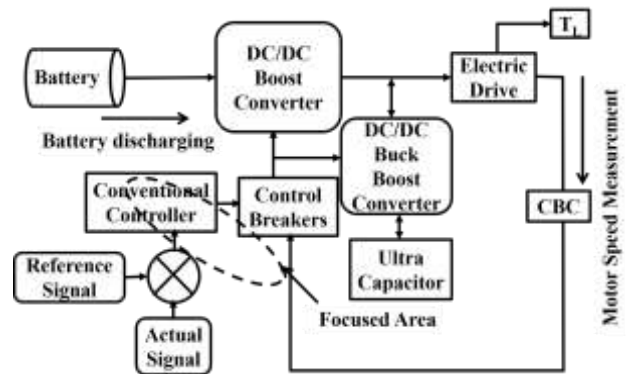


Fig. 1: Representation of the main circuit with all necessary components

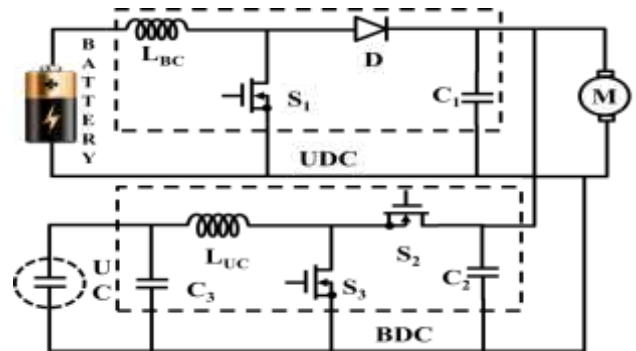


Fig. 2: Main circuit with BDC and UDC including switches

In this circuit, MESS is showing which is comprised of battery and UC which clear in Figure 2. The BDC can operate under boost as well as buck modes. Generally, BDC will act as a medium between load to source and the power flow may be a load to source or source to load related to the applied torque to the motor. On the other hand, UDC also acts as between battery to load and which allows power flow from source to load only. In this work point of view, switches S1, S2, and S3 are corresponding to UDC and BDC. Except during

heavy load and cool starting periods, switch S1 is always in ON condition. In the same way switch, S2 is in ON condition only during no-load periods on the electric motor. At the time of sharing the extra burden on the battery by UC, switch S3 will be in ON condition and during the starting of the electric motor.

3 Different Energy Management Cases based on Load

The main circuit operation in four cases can be represented in the above Figure 3, and for each case, one separate circuit is plotted. In case-1, only switch S3 is in the ON state, to meet the motor requirement due to a heavy load which starts the BDC operation as a boost. During case-2, switches S3, and S1 both are in the enable state, and S2 is in the OFF state. This starts the operation of both converters under boost mode. In case 3, after applying the desired load, the action of the UDC works as boost, and no operation is required from BDC. Finally, no load is applied in the fourth case, due to which the battery is capable of supplying energy to load UC as well. Therefore, during the last case S1, and S2 both are in an ON state to fulfill the load demand.

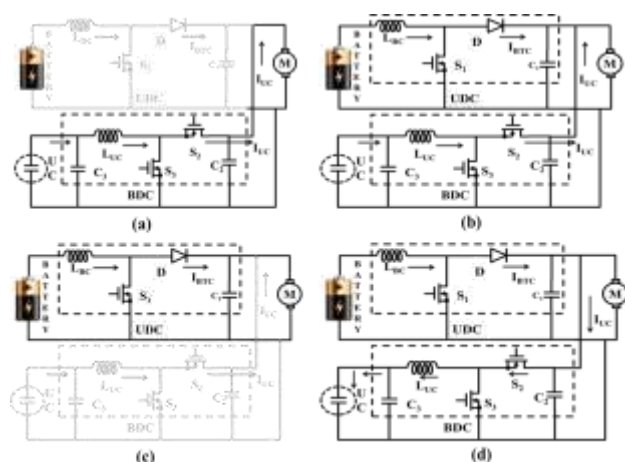


Fig. 3: Main circuit with BDC as well as UDC converters including switches (a) case-1 (b) case-2 (c) case-3 (d) case-4

4 Implementation of Proposed Control Strategy

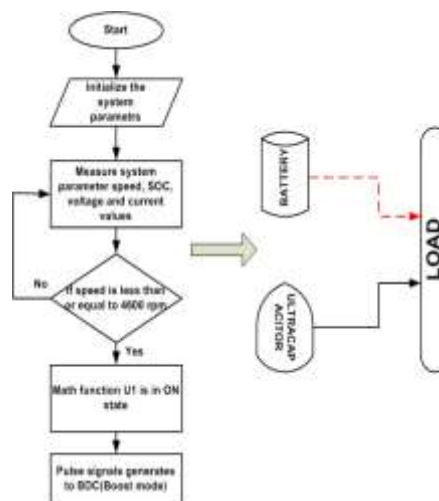
This control strategy mainly consists of two controllers in which the CBC plays a vibrant role to obtain the smooth transition of energy source. On the other hand, a conventional/intelligent controller is required to produce a switching signal related to the load on the motor. Besides, the CBC will send

the controlled signals to the converters according to the vehicle dynamics. The CBC can be realized based on four different speed conditions, which describe the system performance during all load conditions.

4.1 Realizing CBC Controllers with Four Math Functions

The design of the CBC is mainly by considering four math functions separately related to the drive's speed. Different load conditions are considered, and various speed regions are also classified, with all those speed regions, a CBC is considered which is useful to produce the controlled pulse signal to switches existing in BDC and UDC.

- (a) During the first case of operation, the speed of the motor is 4800 rpm due to the huge load applied which initiates output of math function U1 as "1" and "0" for other math functions.
- (b) In the second case, more than a normal load is applied due to that, the speed of the motor maintains between 4600 rpm and 4800rpm. This attempt initiates the math functions U1, and U2 outputs as one and zero for the other two math functions.
- (c) Case three is related to the rated load applied, due to the motor's speed sustained between 4801 rpm to 4930 rpm. Math function U3 only generates an output signal as one and the remaining math functions produce output as zero.
- (d) In the fourth case, the motor's speed is greater than or equal to 4931rpm due to no load applied. Two math functions U1, and U2 generates output as one and the other two U3, and U4 math functions generate output signals as zero.



(a)

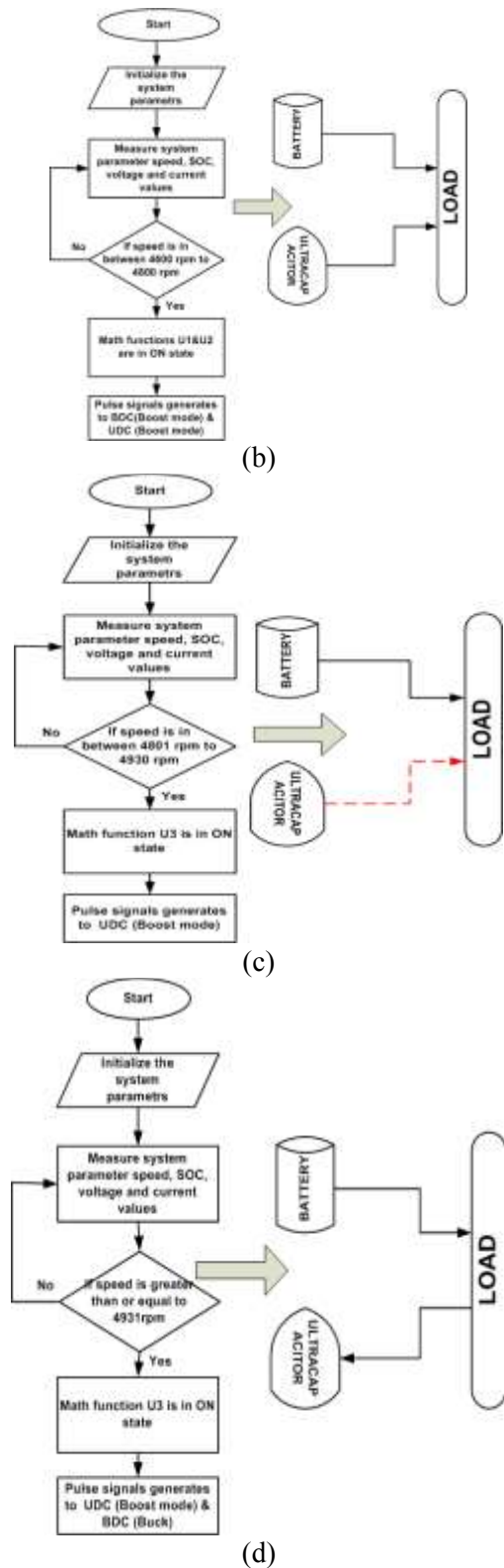


Fig. 4: Flow chart representation of control strategy (a) for case one (b) for case two(c) for case three (d) for case four

Figure 4 (a), (b), (c) and (d) shows the flow chart representation of the four modes of the operation applied with proposed control technique

and which clearly shows the energy sources ON and OFF states of the system.

4.2 Realizing Control Strategy with CBC Controller

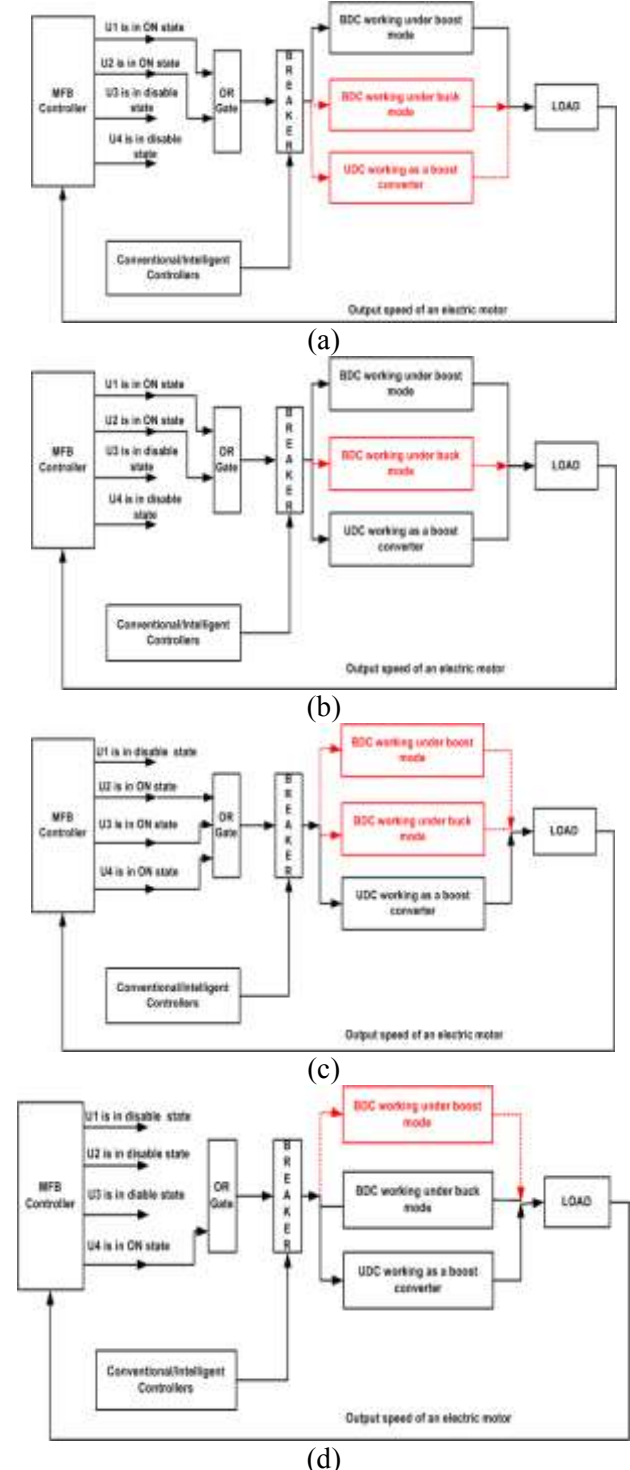


Fig. 5: Pulse signals produced to DC-DC converters by the designed control strategy approach (a) Circuit for BDC operation under boost mode (b) Circuit for UDC as well as BDC operation under boost mode (c) Circuit for UDC operation under boost mode (d) Circuit for BDC (buck) as well as UDC (boost)

Figure 5(a) shows how the pulses are produced to the UDC to propel the EV from the battery only. In this case, no operation is required from the BDC because; the motor is running under rated load. Figure 5(b) shows how the signals are produced to UDC (boost) as well as BDC (boost). Figure 5(c) represents how the signals are produced to UDC (boost). Figure 5(d) shows how the signals are produced to UDC (boost) as well as BDC (buck).

The proposed technique has been modeled based on four outputs of CBC (U1, U2, U3, U4) which are obtained from the input speed of the motor at different load conditions. The objective function is formulated as:

$$U_1, U_2, U_3, U_4 = f(x) \quad (1)$$

$$f(x) = \begin{cases} U_1; x \leq 4800rpm \\ U_1 \& \& U_2; 4600rpm \leq x \leq 4800rpm \\ U_3; 4801rpm \leq x \leq 4930rpm \\ U_4; x \geq 4931rpm \end{cases} \quad (2)$$

5 MATLAB/Simulink Results with Comparison

The MATLAB/Simulink model output results are attained corresponding to four cases of operation based on the motor's speed. Figure 6, Figure 8, Figure 10, Figure 12, Figure 14, Figure 16, Figure 18 and Figure 20 represents the current and speed responses of the motor with CBC plus FLC as well as CBC with PID. In each case corresponding load is applied which creates the distortions in speed as well as current. In the same way Figure 7, Figure 9, Figure 11, Figure 13, Figure 15, Figure 17, Figure 19 and Figure 21 corresponding to how the switching signals are generated during starting and transient periods, all those obtained with different load conditions.

5.1 Case-I

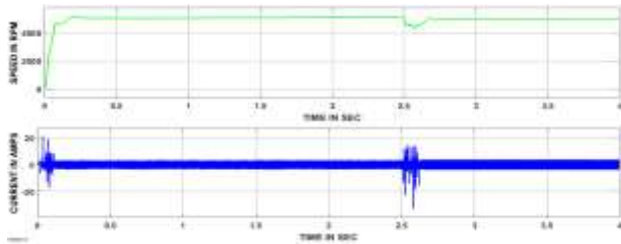


Fig. 6: Output responses of the motor corresponding to CBC with FLC

During starting, the motor draws a huge current to obtain the required speed. In this case, of operation, a heavy load is applied, which causes the rise of current value and decrement of speed up to 0.2 sec. Thereafter motor reached the stable state by the CBC plus FLC.

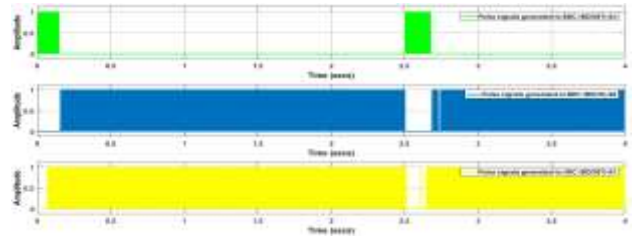


Fig. 7: Representation pulses to BDC and UDC by the CBC with FLC

Figure 7 shows how the controlled switching pulses are producing the DC-DC converts corresponding to vehicle dynamics. During the starting of the motor, the controlled pulses are produced to BDC (boost) up to 0.15 sec. After the motor reaches the normal state, it initiates the production of signals to BDC (buck) and BDC (boost) until load is applied. A heavy load is applied at 2.5 sec, due to that motor speed being reduced, and the current value is raised to 0.2 sec, which starts the process of BDC (boost) and no switching signals to UDC.

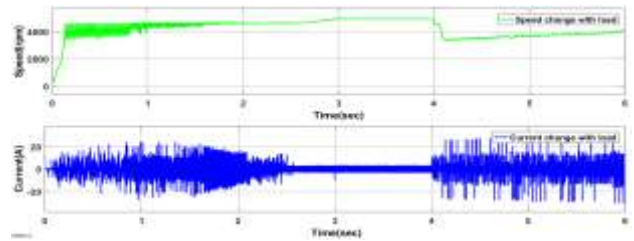


Fig. 8: Output responses of the motor corresponding to CBC with PID

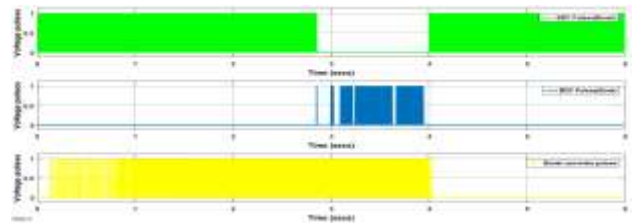


Fig. 9: Representation pulses to BDC and UDC by the CBC with PID

5.2 Case-II

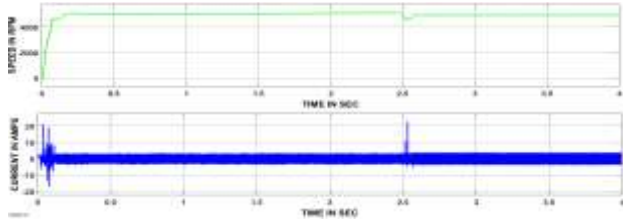


Fig. 10: Output responses of the motor corresponding to CBC with FLC

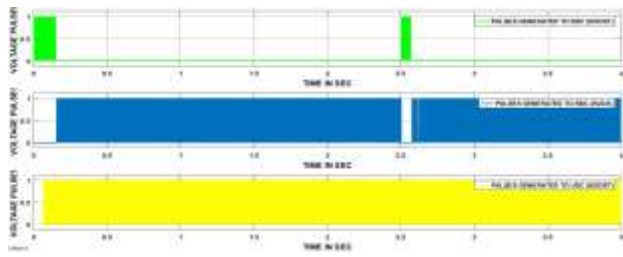


Fig. 11: Representation pulses to BDC and UDC by the CBC with FLC

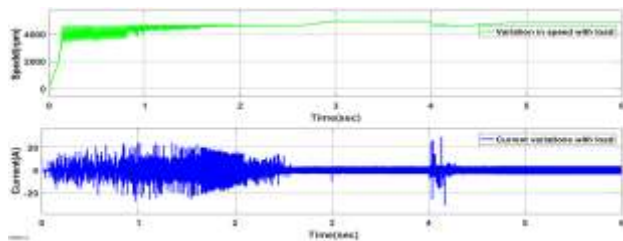


Fig. 12: Output responses of the electric motor corresponding to CBC with PID

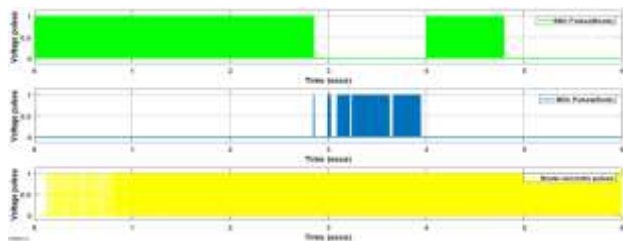


Fig. 13: Representation pulses to BDC and UDC by the CBC with PID

5.3 Case-III

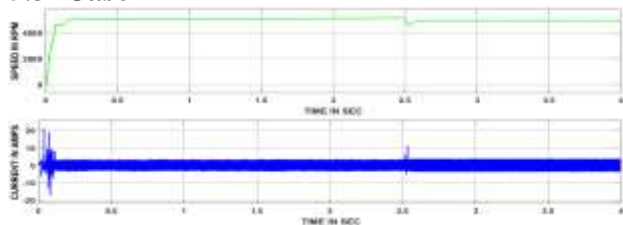


Fig. 14: Output responses of the electric motor corresponding to CBC with FLC

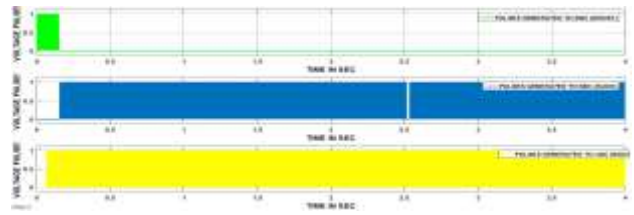


Fig. 15: Representation pulses to BDC and UDC by the CBC with FLC

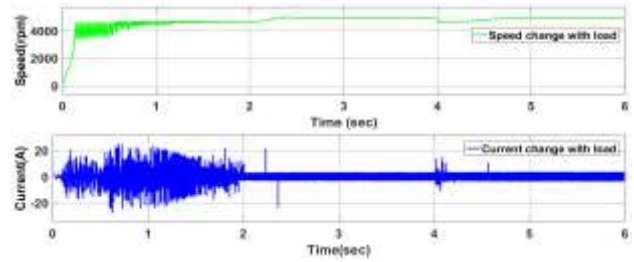


Fig. 16: Output responses of the electric motor corresponding to CBC with PID

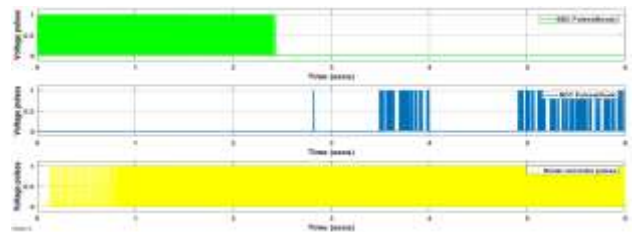


Fig. 17: Representation pulses to BDC and UDC by the CBC with PID

5.4 Case-IV

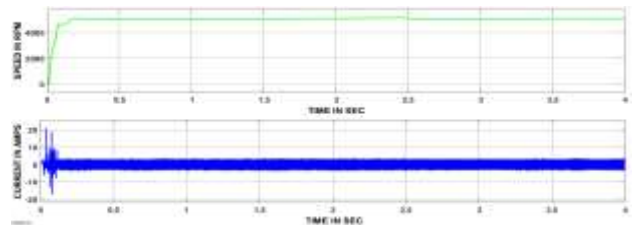


Fig. 18: Output responses of the motor corresponding to CBC with FLC

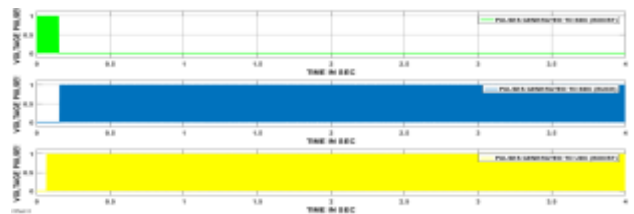


Fig. 19: Representation pulses to BDC and UDC by the CBC with FLC

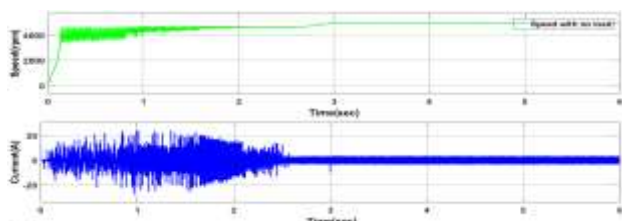


Fig. 20: Output responses of the motor corresponding to CBC with PID



Fig. 21: Representation pulses to BDC and UDC by the CBC with PID

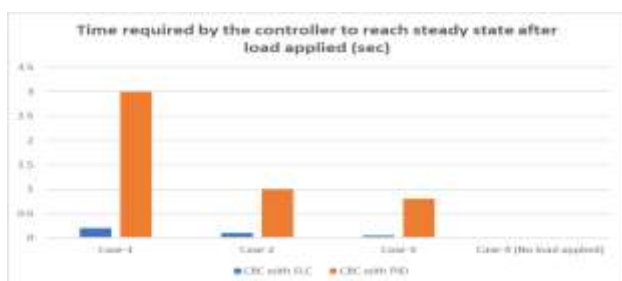


Fig. 22: Representation of a hybrid controller's performance with their steady-state reaching times corresponding to each case

Figure 22 shows that the stable state reaches the time of individual controllers. In the first three cases, CBC with FLC took less time to reach the normal state (maximum time is 0.25 sec and the minimum time is 0.05 sec) whereas CBC with PID took more time to attain the original state (In the first case the wave not settled at normal state, case-2 took 1.2 sec, in case-3 0.8 sec).

6 Conclusions

By combining CBC with the PID/FLC controller, a control strategy has developed to attain the automatic transition between two sources in MESS. For successful operation, the main circuit is simulated in four modes based on various loads. The two-hybrid controllers CBC with FLC, and CBC with PID are realized to the main circuit in all modes of operation and obtain satisfactory results. In case one CBC controller produced switching signals as “1” for the output of CBC U1 and “0” for other outputs, which started the action of BDC as a boost, no pulses are developed to UDC. During case

two, math functions U1, and U2 produced output as one, which started the process of BDC and UDC as a boost. In case three, CBC produced a signal as “1” from outputs U3 and “0” for other math functions, which initiated the operation of UDC as boost, no signals are produced to UDC. During case four, CBC produced output signals as “1” for math function U4 and “0” for other math functions, which begins the operation of BDC (as a buck) and UDC (as boost). Two-hybrid controllers are taken at different times to reach the original state during starting as well as the sudden load applied conditions. Thereafter comparative analysis has been done between the two-hybrid controllers based on the different time domain specifications to identify the performance of the individual controller, those are represented in graph form in the conclusion section.

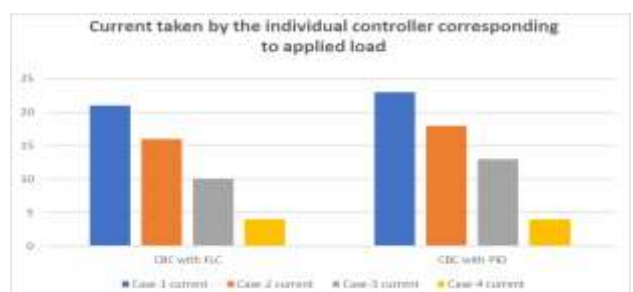


Fig. 23: comparative study between two hybrid controllers corresponding to the current taken by the individual controller, in each case

Figure 23 represents the current taken by the individual controller corresponding to the load applied.

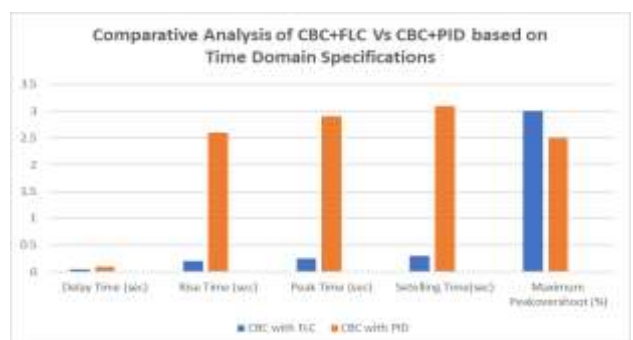


Fig. 24: Performance analysis of hybrid controllers based on time-domain specifications

Figure 24 is the time domain-based comparison between two controllers that are adopted to attain the control objective. Individual controller related time response is represented clearly in the Figure 25.

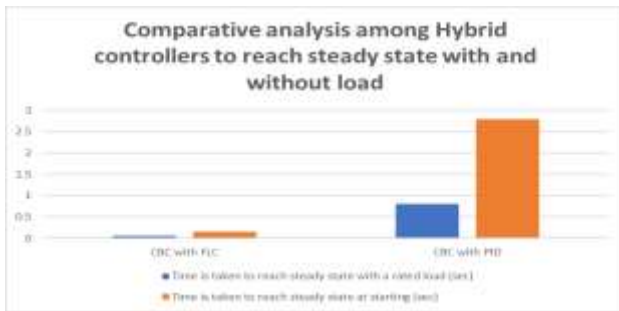


Fig. 25: Steady-state reaching time is taken by the individual controller with and without load

References:

- [1] Shen, J., & Khaligh, A. (2016). Design and real-time controller implementation for a battery-ultracapacitor hybrid energy storage system. *IEEE Transactions on Industrial Informatics*, 12(5), 1910-1918.
- [2] Wu, D., Todd, R., & Forsyth, A. J. (2014). Adaptive rate-limit control for energy storage systems. *IEEE Transactions on Industrial Electronics*, 62(7), 4231-4240.
- [3] Xiang, C., Wang, Y., Hu, S., & Wang, W. (2014). A new topology and control strategy for a hybrid battery-ultracapacitor energy storage system. *Energies*, 7(5), 2874-2896.
- [4] Katuri, R., & Gorantla, S. (2020). Modeling and analysis of hybrid controller by combining MFB with FLC implemented to an ultracapacitor-based electric vehicle. *WSEAS Transactions on Power Systems*, 15, 21-29, <https://doi.org/10.37394/232016.2020.15.3>.
- [5] Khaligh, A., & Li, Z. (2010). Battery, ultracapacitor, fuel cell, and hybrid energy storage systems for electric, hybrid electric, fuel cell, and plug-in hybrid electric vehicles: State of the art. *IEEE transactions on Vehicular Technology*, 59(6), 2806-2814.
- [6] Carter, R., Cruden, A., & Hall, P. J. (2012). Optimizing for efficiency or battery life in a battery/supercapacitor electric vehicle. *IEEE Transactions on Vehicular Technology*, 61(4), 1526-1533.
- [7] Golchoubian, P., & Azad, N. L. (2017). Real-time nonlinear model predictive control of a battery-supercapacitor hybrid energy storage system in electric vehicles. *IEEE Transactions on Vehicular Technology*, 66(11), 9678-9688.
- [8] Gautam, A. K., Tariq, M., Pandey, J. P., Verma, K. S., & Urooj, S. (2022). Hybrid Sources Powered Electric Vehicle Configuration and Integrated Optimal Power Management Strategy. *IEEE Access*, 10, 121684-121711.
- [9] Katuri, R., & Gorantla, S. (2023). Design and comparative analysis of controllers implemented to hybrid energy storage system based solar-powered electric vehicle. *IETE Journal of Research*, 69(7), 4566-4588.
- [10] Akar, F., Tavlasoglu, Y., Ugur, E., Vural, B., & Aksoy, I. (2015). A bidirectional nonisolated multi-input DC-DC converter for hybrid energy storage systems in electric vehicles. *IEEE Transactions on Vehicular Technology*, 65(10), 7944-7955.
- [11] Cao, J., & Emadi, A. (2011). A new battery/ultracapacitor hybrid energy storage system for electric, hybrid, and plug-in hybrid electric vehicles. *IEEE Transactions on power electronics*, 27(1), 122-132.
- [12] Akar, F., Tavlasoglu, Y., & Vural, B. (2016). An energy management strategy for a concept battery/ultracapacitor electric vehicle with improved battery life. *IEEE Transactions on Transportation Electrification*, 3(1), 191-200.
- [13] Masrur, M. A. (2020). Hybrid and electric vehicle (HEV/EV) technologies for off-road Applications. *Proceedings of the IEEE*, 109(6), 1077-1093.
- [14] Dost, P. K. H., Spichartz, P., & Sourkounis, C. (2017). Charging behavior of users utilizing battery electric vehicles and extended range electric vehicles within the scope of a field test. *IEEE Transactions on Industry Applications*, 54(1), 580-590.
- [15] Podder, A. K., Chakraborty, O., Islam, S., Kumar, N. M., & Alhelou, H. H. (2021). Control strategies of different hybrid energy storage systems for electric vehicles applications. *IEEE Access*, 9, 51865-51895.
- [16] Phan, D., Bab-Hadiashar, A., Fayyazi, M., Hoseinnezhad, R., Jazar, R. N., & Khayyam, H. (2020). Interval type 2 fuzzy logic control for energy management of hybrid electric autonomous vehicles. *IEEE Transactions on Intelligent vehicles*, 6(2), 210-220.
- [17] Diao, X., Jiang, L., Gao, T., Zhang, L., Zhang, J., Wang, L., & Wu, Q. (2023). Research on Electric Vehicle Charging Safety Warning based on A-LSTM Algorithm. *IEEE Access*, vol. 11, pp. 55081-55093.
- [18] Sun, Q., Lv, H., Wang, S., Gao, S., & Wei, K. (2021). Optimized state of charge estimation of lithium-ion battery in smes/battery hybrid energy storage system for electric vehicles. *IEEE Transactions on Applied Superconductivity*, 31(8), 1-6.
- [19] Yang, J., Wang, W., Ma, K., & Yang, B. (2019). Optimal dispatching strategy for

shared battery station of electric vehicle by divisional battery control. *IEEE Access*, 7, 38224-38235.

- [20] Alobeidli, K., & Khadkikar, V. (2018). A new ultracapacitor state of charge control concept to enhance battery lifespan of dual storage electric vehicles. *IEEE Transactions on Vehicular Technology*, 67(11), 10470-10481.

Contribution of Individual Authors to the Creation of a Scientific Article (Ghostwriting Policy)

The authors equally contributed to the present research, at all stages from the formulation of the problem to the final findings and solution.

Sources of Funding for Research Presented in a Scientific Article or Scientific Article Itself

No funding was received for conducting this study.

Conflict of Interest

The authors have no conflicts of interest to declare.

Creative Commons Attribution License 4.0 (Attribution 4.0 International, CC BY 4.0)

This article is published under the terms of the Creative Commons Attribution License 4.0

https://creativecommons.org/licenses/by/4.0/deed.en_US